A mutant cholera toxin B subunit that binds GM1-ganglioside but lacks immunomodulatory or toxic activity

A. T. Aman*†, S. Fraser*†, E. A. Merritt‡, C. Rodigherio*§, M. Kenny*, M. Ahn‡, W. G. J. Hol‡¶, N. A. Williams*, W. I. Lencer§, and T. R. Hirst*‖

*Department of Pathology and Microbiology, University of Bristol, Bristol BS81TD, United Kingdom; ‡Department of Structural Biology and ¶Howard Hughes Medical Institute, University of Washington, Seattle, WA 98195; and §Combined Program in Pediatric Gastroenterology and Nutrition, Children's Hospital, Boston, MA 02115

Communicated by Linda L. Randall, University of Missouri, Columbia, MO, May 31, 2001 (received for review February 6, 2001)

GM1-ganglioside receptor binding by the B subunit of cholera toxin (CtxB) is widely accepted to initiate toxin action by triggering uptake and delivery of the toxin A subunit into cells. More recently, GM1 binding by isolated CtxB, or the related B subunit of *Escherichia coli* heat-labile enterotoxin (EtxB), has been found to modulate leukocyte function, resulting in the down-regulation of proinflammatory immune responses that cause autoimmune disorders such as rheumatoid arthritis and diabetes. Here, we demonstrate that GM1 binding, contrary to expectation, is not sufficient to initiate toxin action. We report the engineering and crystallographic structure of a mutant cholera toxin, with a His to Ala substitution in the B subunit at position 57. Whereas the mutant retained pentameric stability and high affinity binding to GM1-ganglioside, it had lost its immunomodulatory activity and, when part of the holotoxin complex, exhibited ablated toxicity. The implications of these findings on the mode of action of cholera toxin are discussed.

Cholera toxin (Ctx) and its close homologue, the heat-labile enterotoxin of *Escherichia coli* (Etx), are hexameric AB_5 toxins responsible for causing profuse and, at times, life-threatening diarrheal disease (for review, see refs. 1 and 2). Their toxicity is attributable to the enzymatic activity of the A subunit, which catalyzes ADP-ribosylation of the α-subunit of the trimeric GTP-binding protein, G_s, leading to activation of adenylate cyclase and a concomitant elevation in cAMP levels. The five B subunits of these toxins, which bind predominantly to GM1 ganglioside [Gal(β1-3)GalNAc(β1-4){NeuAc(α2-3)}Gal(β1-4)Glc(β1-1)ceramide] receptors found on the surface of mammalian cells, are widely thought of as delivery vehicles for the A subunit (3, 4). However, recent studies on the immunological properties of cholera toxin B subunit (CtxB) and *E. coli* enterotoxin B subunit (EtxB) have shown that they can trigger signaling events in their own right, which alter leukocyte differentiation, survival, and death (5) (R. Salmond, T.R.H., and N.A.W., unpublished observations). One of the most unexpected and striking effects of the B subunits is their capacity to trigger the selective apoptosis of $CD8^+$ T cells, as well as to alter $CD4^+$ T-cell differentiation, activate B cells, and modulate antigen processing and presentation by macrophages (5). These potent immunological properties have led to testing of the B subunits as adjuvants for stimulating mucosal and systemic responses to coadministered antigens (6, 7) and as agents for down-regulating proinflammatory autoimmune diseases such as rheumatoid arthritis and diabetes (8–10).

The importance of receptor binding by the B subunits in triggering both toxin action on epithelial cells and in modulating immune cell function has been established by the use of mutant B subunits that do not bind GM1, namely EtxB(G33D) and CtxB(G33E). Such mutants fail to modulate leukocyte function *in vitro* or elicit a potent immune response *in vivo* (11–14), and the corresponding mutant holotoxins fail to trigger Cl^- secretion by T84 cells. What is not yet clear is how the binding of the B subunits to receptors such as GM1 can trigger signal transduction or induce toxin internalization. It may be that the pentameric crosslinking of GM1 causes local alterations in membrane dynamics and the microlipid environment, which in turn influences the activity of integral membrane proteins that participate in cell signaling. In this regard, GM1 appears to be preferentially located in cholesterol-rich membrane microdomains (15, 16) that contain a high concentration of signaling molecules (17). Another possibility is that high affinity binding of the B subunits to GM1 permits their direct lower affinity interaction with cell-surface signaling proteins. Because both CtxB and EtxB have the same properties, such a cognate protein–protein interaction would have to be conserved within the structure of the two molecules. Interestingly, CtxB and EtxB contain an extensive conserved segment spanning residues 45 to 74 that contains an exposed loop from Val-52 to Ile-58 located on the lower convoluted surface of the molecule (1, 4). This is normally oriented toward the cell membrane and forms part of the GM1-binding surface, with residues Gln-56, His-57, and Ile-58 involved in a network of solvent-mediated hydrogen bonds that is conserved in the presence of bound GM1-pentasaccharide (18, 19).

To investigate whether this region of the B subunits is important for toxin action in disease and in B subunit-mediated immunomodulation, the individual residues of the loop were sequentially substituted for Ala. Here, we show that one of the mutants, with a His to Ala substitution at position 57 [CtxB(H57A)], is severely defective as an immunomodulator and that the corresponding holotoxin, Ctx(H57A), exhibits ablated toxicity even though these molecules retain the ability to bind with high affinity to GM1. X-ray crystallographic analysis of CtxB(H57A) revealed that the loop region had undergone a striking 7-Å shift, partially occluding the pore region on the lower convoluted surface of the molecule, while not altering the capacity of the receptor pocket to cocrystallize with galactose. This indicates that the loop defines an important site on cholera toxin that is essential for its diverse activities and that GM1 binding alone is not sufficient to trigger toxin action.

Materials and Methods

Alanine-Scanning Mutagenesis and Gene Manipulation. Ala substitutions were introduced into the Val-52 to Ile-58 loop of CtxB by

Abbreviations: Ctx, cholera toxin; Etx, enterotoxin; OS, oligosaccharide.

Data deposition: The atomic coordinates have been deposited in the Protein Data Bank, www.rcsb.org (PDB ID code 1g8z).

†T.A. and S.F. contributed equally to this work.

‖To whom reprint requests should be addressed. E-mail: t.r.hirst@bristol.ac.uk.

The publication costs of this article were defrayed in part by page charge payment. This article must therefore be hereby marked "*advertisement*" in accordance with 18 U.S.C. §1734 solely to indicate this fact.

PCR mutagenesis (20). Plasmid pATA14 (21), a pBluescript IIKS derivative containing a reconstructed *ctxAB* operon with an engineered *Eco*RI site at the 3′ end of the *ctxA* gene, was used as a PCR template. PCR fragments, with appropriately engineered substitutions in *ctxB*, were ligated into the *Eco*RI–*Spe*I sites of pATA14, thereby replacing the wild-type *ctxB* gene with a mutant allele. The resultant plasmids, pATA16 to pATA22, were confirmed by DNA sequencing to encode Ala substitutions at residues 52–58 in CtxB, respectively.

Plasmid pCDR3 was constructed by subcloning the *Eco*RV–*Spe*I fragment containing the entire *ctxAB* operon of pATA14 into the controlled expression vector pTTQ18 (21).

To facilitate subsequent purification and characterization of wild-type and mutant B subunits (devoid of any A subunit), the *ctxB* gene from pATA14 and the mutant *ctxB* allele of pATA21 were subcloned into *Eco*RI–*Spe*I digested pTRH64 (13), a broad host range controlled expression vector derived from pMMB66EH (22). The resultant plasmids were designated pATA13, encoding wild-type CtxB, and pATA29, encoding the mutant B subunit CtxB(H57A).

Periplasmic Extraction. Periplasmic extracts from *E. coli* XL1-Blue (Stratagene) harboring plasmids pATA14 or pATA16 to pATA22 were prepared as described in ref. 23 and immediately dialyzed against HBSS (Sigma) containing 10 mM Hepes pH 7.4, then flash frozen and stored at −80°C before electrophysiologic analysis.

Purification of Proteins. Plasmids pCDR3 and pATA21 encoding Ctx holotoxin and Ctx holotoxin [with an H57A mutation in the B subunit (Ctx(H57A)], respectively, were electroporated into *Vibrio cholerae* 0395NT (which contains an engineered chromosomal *ctxAB* deletion), and the toxins were purified as reported (21). Plasmids pATA13 and pATA29 encoding wild-type CtxB and CtxB(H57A), respectively, were mobilized into the nonpathogenic *Vibrio* sp. 60 strain, and the B subunits were purified from the culture media by using the method reported in ref. 7. EtxB(G33D) was purified from *Vibrio* sp. 60 (pTRH64) as reported (13). Purified B subunit preparations were applied to a detoxigel column (Pierce), and the eluted fractions were pooled and dialyzed against PBS. Protein concentration was determined as reported in ref. 24, and LPS content was shown to be >30 EU/mg^{-1} protein (BioWhittaker).

Crystallographic Structure Determination. Crystals of CtxB(H57A) were grown from hanging drops by vapor diffusion equilibration against a well buffer solution containing 50 mM NaCl/100 mM Tris·HCl, pH 8.4/32% (wt/vol) PEG 5000. Drops consisted of 1 μl of protein at 3 mg/ml in 100 mM Tris·HCl, pH 7.5/1 μl of 300 mM galactose (β-D-galactopyranoside)/1 μl of well buffer. Crystals formed in space group $P2_12_12$ (a = 101.4Å, b = 114.7Å, c = 45.6Å) with one pentamer per asymmetric unit. Diffraction intensities to 2.0 Å resolution were measured from a single flash-frozen crystal by using 12 keV radiation from APS beamline 19ID and a 3K × 3K CCD detector in binned mode. The initial crystallographic model consisted of the previously determined CtxB(H94R) structure (ref. 25; Protein Data Bank accession code 3chb) positioned by molecular replacement. After rigid body refinement of the constituent monomers, the model for residues 50–62 of each subunit was rebuilt manually. Iterative positional and B factor refinement, alternating with manual refitting, yielded crystallographic residuals $r = 0.253$ and $R_{free} = 0.317$. At this point, difference density for bound galactose was clear in two of the five subunits. Continued refinement with incremental addition of discrete water molecules and two additional galactose molecules yielded a model with $r = 0.191$ and $R_{free} = 0.252$. The final stages of refinement included 446 discrete water molecules, 4 galactose molecules, and a riding hydrogen model, yielding final crystallographic residuals $r = 0.179$ and $R_{free} = 0.239$ with excellent stereochemistry. The mean estimated standard uncertainty in atomic coordinates based on Cruickshank's DPI measure was 0.19 Å. Intensity data were merged and scaled by using programs DENZO, SCALEPACK, and TRUNCATE (26, 27). Model fitting and real-space optimization used the program XFIT (28), whereas all remaining refinements used the program REFMAC (27). Figures were prepared by using programs MSMS (29) and RASTER3D (30).

Electrophysiology. T84 cells (from passage 80) obtained from the ATCC were grown and passaged as described (31). Toxins were diluted in prewarmed HBSS (Sigma) and 10 mM Hepes, pH 7.4, and applied to the apical surface of confluent T84 cell monolayers in Transwell inserts (Costar), followed by incubation at 37°C. Measurements of short circuit current (I_{sc}) and resistance (R) were performed as reported elsewhere (31).

Toxin–Receptor Interaction. *GM1-ELISA.* Toxin B subunit interaction with GM1 was monitored on microtiter plates (Immulon 1, Dynatech) coated with 1.5 μg/ml GM1 (Sigma) in PBS as reported (13), using LT39 (32), a monoclonal antibody that detects both CtxB and EtxB, or 118-8, a monoclonal antibody that detects EtxB (33).

Surface Plasmon Resonance. Liposomes were prepared from 2 ml of 5 mol % GM1/95 mol % 1-palmitoyl-2-oleoyl-sn-glycero-3-phosphocholine in chloroform/methanol (2:1). The glycolipid:lipid mixture was allowed to evaporate under vacuum and then dissolved in PBS and passed through a polycarbonate filter (50-nm pore size) using the LipoFast basic system (Avestin, Ottawa) as recommended by the manufacturer and described by Kuziemko *et al.* (34). A BIAcore 1000 (Amersham Pharmacia) was used to coat an HPA sensor chip (BIAcore, Herts, England) with GM1-containing liposomes, and B subunit K_D binding measurements were obtained as reported (34).

Lymphocyte Isolation and Culture. Mesenteric lymph nodes and spleens were removed from 6–10-week-old NIH mice bred under specific pathogen-free (SPF) conditions (University of Bristol), and the tissues were crushed under wire mesh. The cells were then washed three times in Hanks medium without calcium and magnesium (GIBCO/BRL) + 20 mM Hepes (Sigma-Aldrich). Red blood cells were lysed by the addition of 0.5 ml of Ack lysing buffer (BioWhittaker) for 30 s. For the purification of specific lymphocyte populations, cells were washed in PBS containing 0.5% (wt/vol) BSA and 5 mM EDTA (BDH), before the addition of specific antibodies conjugated with MACS microbeads (Miltenyi Biotec, Auburn, CA) for 35 min on ice. $CD8^+$ T cells were negatively selected by using anti-CD4 and anti-B220. B cells were negatively selected by using anti-CD43. Labeled cell suspensions were applied to VS selection columns (Miltenyi Biotec), and the negative fractions were eluted with 0.5% (wt/vol) BSA–PBS containing 5 mM EDTA and used immediately.

MLN cells, purified $CD8^+$ T cells, and B cells were cultured at 37°C in 5% CO_2 at a concentration of 2×10^6/ml in α-modified Eagle's medium (GIBCO) for MLN and $CD8^+$ T cells and RPMI 1640 medium (GIBCO) for B cells, both supplemented with 20 mM Hepes/4 mM L-glutamine/100 units/ml penicillin/100 μg/ml Streptomycin, 5×10^{-5} M 2-mercaptoethanol/5% (vol/vol) FCS (Sigma). MLN and B cells were cultured for 48 h, or $CD8^+$ T cells for 18 h, in the absence or presence of either wild-type or mutant B subunits at the concentrations specified. In some experiments, treated cells were resuspended in Hanks medium supplemented with 20 mM Hepes/0.02% (wt/vol) sodium azide/10% (vol/vol) rat serum and either incubated for 30 min on ice with rat anti-mouse CD8α-PE (PharMingen) and rat anti-mouse CD4-FITC

(PharMingen) or stained with propidium iodide (Sigma) and then analyzed by flow cytometry, as described (14).

Immunfluorescent Staining. Isolated $CD8^+$ T cells (2×10^6) were incubated on ice in PBS with 100 nM wild-type or mutant B subunits for 1 h. Treated cells were analyzed by immunofluorescence microscopy and flow cytometry to detect bound B subunit. For immunofluorescence microscopy, treated cells were washed in ice-cold PBS, overlaid onto cover slips precoated with poly L-lysine (Sigma), fixed [3.7% (vol/vol) formaldehyde, 4°C, 4 min; methanol, −20°C, 5 min], and labeled with anti-EtxB or anti-CtxB antibodies, followed by FITC-goat anti-mouse IgG (Dako). The cover slips were mounted by using Mowiol mounting medium + 2.5% (wt/vol) DABCO (Sigma) and analyzed by using a Zeiss Axioskop fluorescence microscope. In a parallel experiment, the cells were labeled with the same antibodies and analyzed by flow cytometry.

Immunizations. NIH mice were immunized by s.c. immunization with either 2×30 μg of B subunit or intranasal immunization with 3×10 μg of B subunit and anti-CtxB responses were determined by using GM1 microtiter plates coated with 1 μg/ml CtxB as reported (13).

Results and Discussion

Alanine-Scanning Mutagenesis of the Conserved Val-52 to Ile-58 Loop in Cholera Toxin B Subunit. Residues Val-52 to Ile-58 of the B subunit of cholera toxin were subjected to alanine-scanning mutagenesis to assess whether this region, which comprises a conserved, flexible loop, plays an important role in cholera toxin action. To facilitate the construction and analysis of the various mutant Ctx proteins, the *ctxA* and *ctxB* genes were first PCR amplified as separate cistrons and then ligated to reconstruct a *ctx* operon with a conveniently situated *Eco*RI site at the fusion junction. As a consequence, a Lys to Arg substitution was introduced at residue 237 in the mature CtxA subunit, resulting in an alteration in the C-terminal −KDEL sequence, to yield −RDEL (which is identical to the C terminus normally found in the A subunit of *E. coli* enterotoxin). This substitution in CtxA was demonstrated not to alter the A subunit's intrinsic ADP-ribosyltransferase activity or the kinetics and magnitude of toxin-induced Cl^- secretion in polarized T84 epithelial cells (21).

Plasmid pATA14, encoding $CtxA^{(RDEL)}CtxB$ (hereafter referred to as Ctx), was subjected to site-directed mutagenesis to introduce individual Ala substitutions at residues from Val-52 to Ile-58 in CtxB, as described in *Materials and Methods*. When crude periplasmic extracts from *E. coli* strains expressing these mutant Ctx toxins were evaluated for their capacity to induce Cl^- secretion by T84 cells, it was found that one of the mutants containing a His to Ala substitution at residue 57 had an apparent severe toxicity defect (see below). To further investigate this and in particular to evaluate the impact of the H57A mutation on B subunit function, both the mutant holotoxin, Ctx(H57A) and recombinant B subunit, CtxB(H57A), devoid of contaminating A subunit, were purified, and their identities were confirmed by mass spectrometry. Before assessing the functional properties of the mutants, we showed that the intrinsic stability of the CtxB(H57A) pentamers were, like wild-type CtxB, remarkably stable, retaining their oligomeric structure at pH levels as low as 3.0 or when incubated in the presence of 10% (wt/vol) of the ionic detergent, SDS (data not shown).

Ctx(H57A) Exhibits a Severe Defect in Toxicity. Purified preparations of both wild-type Ctx and Ctx(H57A) were tested for their ability to trigger chloride efflux in polarized human intestinal epithelial (T84) cells (Fig. 1). Addition of 2 nM Ctx to the apical surface of T84 cells resulted in a characteristic 40-min lag period followed by rapid and maximal Cl^- efflux, as monitored by a change in short circuit current across the cell monolayer. By contrast, the addition of an equimolar concentration of Ctx(H57A) to T84 cells failed to trigger Cl^- efflux, suggesting that the His-57 residue plays a vital role in cholera toxin action (Fig. 1). The mutant displayed an almost complete lack of toxicity even at concentrations of 1,000 nM (data not shown).

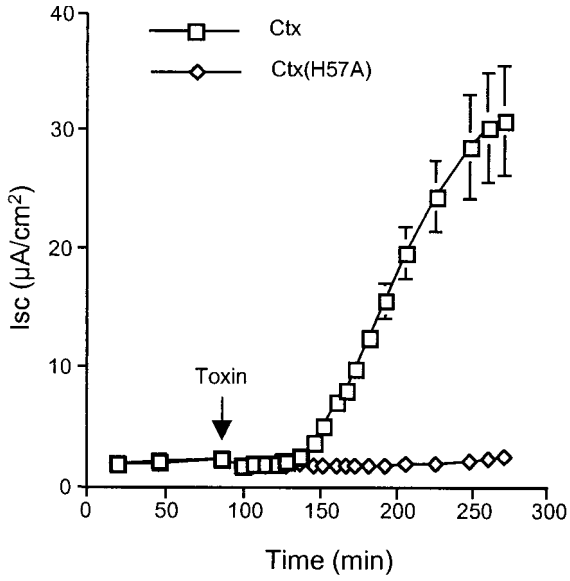

Fig. 1. Ctx(H57A) exhibits a severe defect in toxicity. Time course of electrogenic Cl^- secretion induced by the addition of 2 nM Ctx (□) or Ctx(H57A) (◇) to the apical surface of T84 cell monolayers (with data points representing the mean ± SE, where $n = 2$ independent monolayers). Three independent experiments gave similar results.

CtxB(H57A) Retains the Ability to Bind to GM1 and to the Surfaces of Mammalian Cells. Given that the mutation is adjacent to the receptor-binding pocket in the B subunit, one possible explanation for the toxicity defect was that the mutant had lost the ability to bind with high affinity to GM1-ganglioside.

The binding of CtxB(H57A) to GM1 was evaluated by both ELISA and surface plasmon resonance. Microtiter plates coated with GM1 were incubated with various concentrations of CtxB, CtxB(H57A), and EtxB(G33D), and bound protein was detected by using anti-B subunit monoclonal antibodies (Fig. 2). CtxB and CtxB(H57A) bound to GM1-coated microtiter plates to a similar extent, with the sensitivity of detection for both subunits being in the 1–2 ng/ml range (equivalent to $1.6–3.2 \times 10^{-11}$ M).

The K_D for interaction with GM1 was determined by surface plasmon resonance using the method of Kuziemko *et al.* (34) and found to be 1.9 ($\pm$0.9) $\times 10^{-10}$ M for CtxB and 5.0 ($\pm$3.7) $\times 10^{-10}$ M for CtxB(H57A). We therefore conclude that CtxB(H57A) retains a very high avidity for interaction with GM1.

To further investigate aspects of the function of CtxB(H57A), we assessed whether it could bind to mammalian cells. For this purpose, we selected murine $CD8^+$ T cells, as these had previously been shown to be suitable for assessing CtxB and EtxB-mediated effects on immune cells (14). Highly purified $CD8^+$ T cells from the mesenteric lymph node (MLN) of NIH mice were incubated on ice with 100 nM CtxB, CtxB(H57A), or EtxB(G33D), and the bound B subunits were detected by using anti-B subunit antibodies and an FITC secondary antibody before analysis by fluorescence microscopy (Fig. 3*A*) or flow cytometry (Fig. 3*B*).

Microscopy revealed a clear halo of fluorescence around the cells incubated with both CtxB and CtxB(H57A) but not with

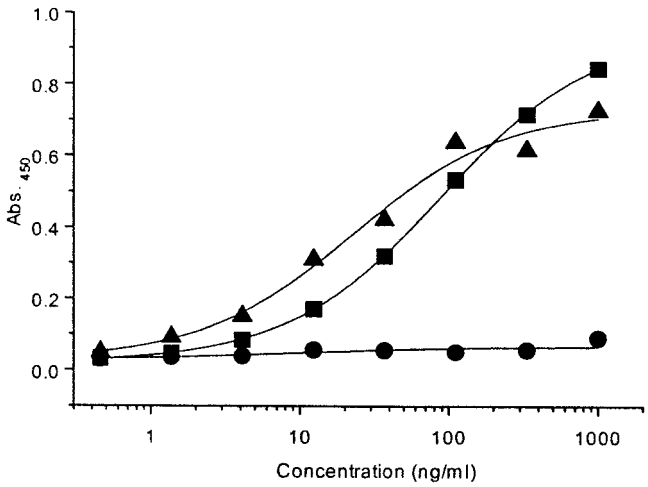

Fig. 2. CtxB(H57A) retains the ability to bind to GM1. CtxB (■), CtxB(H57A) (▲), or EtxB(G33D) (●) at a concentration of 1 μg/ml was serially diluted 3-fold in GM1-coated microtiter plates, and the bound B subunits were detected by immunoassay as described in *Materials and Methods*. Three independent experiments gave similar results.

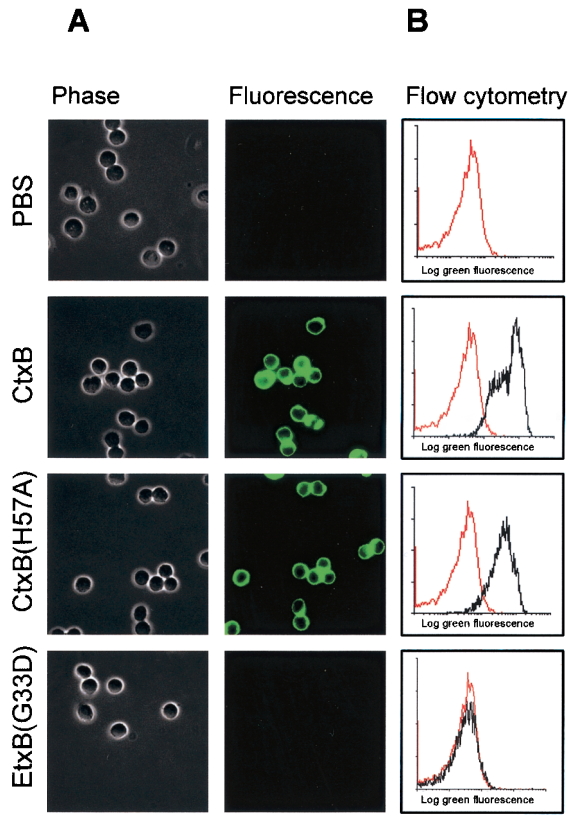

Fig. 3. CtxB(H57A) interaction with CD8$^+$ T cells. Isolated CD8$^+$ T cells derived from the MLN were incubated on ice for 1 h in the absence (PBS control) or presence of 100 nM CtxB, CtxB(H57A), or EtxB(G33D) and then labeled with either anti-CtxB or anti-EtxB antibodies followed by a goat anti-mouse IgG-FITC secondary conjugate. Cells were analyzed by fluorescence microscopy (*A*) or flow cytometry (*B*). The flow cytometric trace obtained for PBS-treated cells is shown in red, and the trace obtained for cells treated with the various B subunits is overlaid in black.

EtxB(G33D) or cells incubated with PBS. Flow cytometry permitted a semiquantitative measurement of B subunit binding to the cells, as the fluorescence detected by the FACscan is directly proportional to the amount of bound secondary antibody. When control samples, using cells incubated in PBS, were analyzed by the FACScan, low-level background fluorescence was detected and is shown as the red line in Fig. 3*B*. Incubation with CtxB and CtxB(H57A), but not with EtxB(G33D), resulted in a marked increase in fluorescence intensity, indicative of B subunit binding to CD8$^+$ T cells (Fig. 3*B*, black line). In addition, when concentrations as low as 1–10 nM were tested, no difference in the relative fluorescence shifts between wild-type CtxB and CtxB(H57A) was observed. We therefore conclude that CtxB(H57A) retains a high affinity for GM1 and shows a comparable level of binding to mammalian cells as wild-type CtxB.

CtxB(H57A) Lacks Immunomodulatory Activity. An unexpected property of CtxB and EtxB is their capacity to induce the selective apoptosis of murine CD8$^+$ T cells, involving an NFκB-dependent and caspase-3-dependent pathway (ref. 14; R. Salmond, T.R.H., and N.A.W., unpublished observations). This has previously been proposed to be dependent on B subunit interaction with GM1, as EtxB(G33D) fails to elicit such an effect (14). CtxB(H57A) was therefore tested to assess whether it had retained the capacity to induce CD8$^+$ T cell apoptosis. MLN cells were cultured for 48 h in the presence or absence of 100 nM CtxB, CtxB(H57A), or EtxB(G33D), and then the CD4$^+$ and CD8$^+$ T cells were stained with fluorescently labeled antibodies and detected by flow cytometry. Fig. 4*A* shows that after 48 h, cells cultured with either PBS or the nonbinding mutant EtxB(G33D) contained $\approx$17–18% CD8$^+$ T cells, whereas treatment with wild-type CtxB reduced the proportion of CD8$^+$ T cells to $<$6%. Strikingly, CtxB(H57A) failed to induce any CD8$^+$ T cell depletion above that seen for the negative controls. To investigate this further, MLN cell cultures were treated with concentrations of B subunit ranging from 10 nM to 2.5 μM, and CD8$^+$ T cell depletion was assessed as before (Fig. 4*B*). This revealed that 100 nM CtxB resulted in maximal CD8$^+$ T cell depletion, whereas even at the highest concentration of 2.5 μM, CtxB(H57A) showed only a modest capacity to induce depletion. High doses of the B subunits (3.45 μM) were also tested for their capacity to induce apoptosis in isolated CD8$^+$ T cells derived from the MLN. The cells were cultured for 18 h in the presence or absence of the B subunits and then stained with propidium iodide to reveal levels of subdiploid DNA, indicative of apoptotic cells. Fig. 4*C* shows that wild-type CtxB, but not CtxB(H57A) or EtxB(G33D), increased the percentage of apoptotic cells above background. We therefore conclude that, even though CtxB(H57A) binds to CD8$^+$ T cells, it nonetheless exhibits a severe defect in inducing their apoptosis.

In addition, the effect of CtxB and the mutant B subunits on activation of B cells was investigated as it has been reported that CtxB and EtxB cause the up-regulation of MHC class II and CD25 (11, 12). As expected, 48-h treatment of isolated splenic B cells with 1.75 μM CtxB increased surface expression of MHC class II and CD25, whereas CtxB(H57A) or EtxB(G33D) did not (data not shown).

To investigate whether the defect in modulation of immune cells *in vitro* correlated with a corresponding loss in potent immunogenicity *in vivo*, mice were immunized s.c. or intranasally with CtxB or CtxB(H57A) as described in *Materials and Methods*. Subcutaneous immunization with 30 μg of CtxB or CtxB(H57A) in PBS, on two occasions 10 days apart, resulted in a 78-fold difference in mean serum anti-B subunit IgG titers of 7,000 $\pm$ 1,800 and 90 $\pm$ 90, respectively. If mice were given three 10-μg intranasal doses of CtxB or CtxB(H57A) in PBS, on three occasions 7 days apart, the mean serum anti-B subunit titers were 125,000 $\pm$ 64,000 and 11,000 $\pm$ 3,000, respectively. We therefore

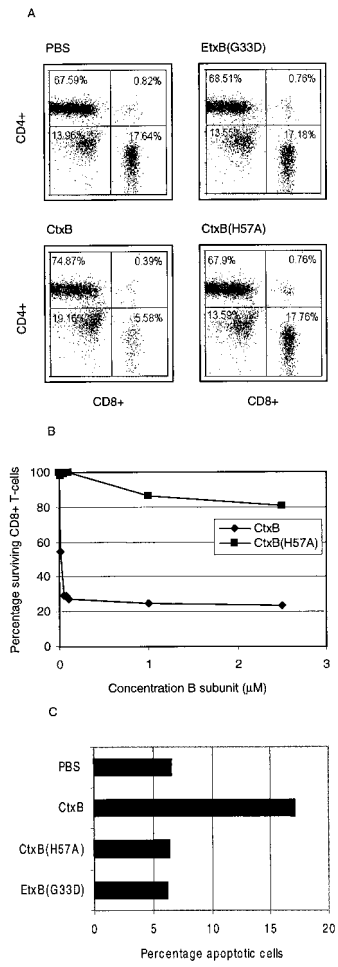

Fig. 4. CtxB(H57A) is defective in triggering $CD8^+$ T cell apoptosis. (*A*) MLN cells were cultured for 48 h in the absence (PBS control) or presence of 100 nM CtxB, CtxB(H57A), or EtxB(G33D) and then stained with anti-CD8(PE) and anti-CD4(FITC) antibodies and analyzed by flow cytometry. The percentage of $CD8^+$ T cells is shown in the lower right hand quadrant. (*B*) MLN cells were cultured in the presence of CtxB or CtxB(H57A) at concentrations ranging from 10 nM to 2.5 μM and labeled and analyzed as above. The percentage of surviving $CD8^+$ T cells, compared with PBS-treated control cells, was calculated. (*C*) Isolated $CD8^+$ T cells derived from the MLN were cultured for 18 h in the absence (PBS control) or with 3.45 μM CtxB, CtxB(H57A), or EtxB(G33D) and then stained with propidium iodide and analyzed by flow cytometry to determine the percentage of cells containing subdiploid DNA.

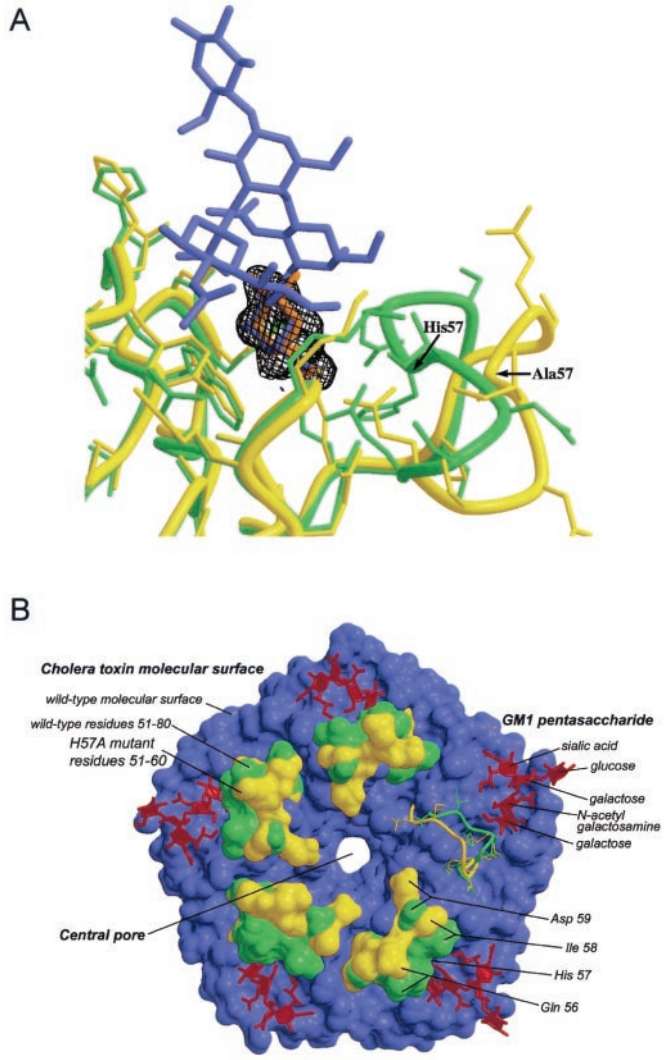

Fig. 5. Superimposed crystal structures of wild-type CtxB and CtxB(H57A). (*A*) Superposition of the crystal structure of wild-type CtxB (green) complexed with GM1-OS (blue) onto the structure of the CtxB(H57A) mutant (yellow) complexed with galactose (red). A single receptor-binding site (site H) of the five independent sites is shown. Electron density for the galactose molecule is shown at 2σ contours in an (mF_{obs}-F_{calc}) omit map. The point of maximal difference between the peptide backbones of the wild-type and mutant toxins is at residue Gln-56, where the respective C^{α} atom positions differ by 7 Å. (*B*) Superposition of the wild-type cholera toxin B pentamer in complex with the receptor oligosaccharide onto the CtxB(H57A) mutant B pentamer. The molecular surface of wild-type CTB is shown in green (50–60 loop) and blue. The GM1-oligosaccharide is shown in red. The molecular surface of the H57A mutant is shown in yellow (50–60 loop). The terminal galactose residue of the GM1-oligosaccharide is not visible behind the molecular surface of the 50–60 loop, which forms one side of its binding site on the protein. At one of the five binding sites, the molecular surface of this loop is not shown so that the underlying protein conformation may be seen.

conclude that the H57A mutation causes a marked reduction in B subunit immunogenicity.

X-Ray Crystallographic Structure of CtxB(H57A). To gain an insight into the structural consequences of substituting His-57, CtxB(H57A) was cocrystallized with galactose. This revealed an x-ray structure that is remarkable in several respects. The most striking alteration is the conformation of the Val-52–Ile-58 loop in CtxB(H57A), which is quite different from that found in the wild-type toxin (Fig. 5). The C^{α} atom of the mutated residue 57 is shifted by ≈4 Å, and the difference in the backbone position increases to ≈7 Å at residue Gln-56 in comparison with the structure of wild-type CtxB complexed with GM1-oligosaccharide (GM1-OS) (18, 25). Moreover, the shift is observed in all five subunits, even though galactose is bound only to four of them. The net effect of the conformational change is to displace residues 52–58 toward the central pore of the toxin B-pentamer, with the result that the accessible surface of the toxin pentamer is substantially altered in this region (Fig. 5*B*). In the wild-type CtxB:GM1-OS complex, both residues Glu-51 and Gln-61 form direct hydrogen bonds with the terminal galactose of GM1, whereas residue Gln-56 forms solvent-mediated hydrogen bonds with both the terminal galactose and the sialic acid of GM1. Given this, it is somewhat unexpected that such a large change in loop conformation does not disrupt, or at least perturb, sugar binding. Nevertheless, the observed galactose location in the present complex differs by only 0.4 Å rms from that seen for the

terminal galactose in the GM1-OS complex (Fig. 5*A*). We therefore would predict that regardless of the displacement of the loop, the overall GM1 binding mode is essentially unperturbed by the mutation (Fig. 5*B*), which is in accord with our biophysical measurements of GM1 affinity.

In addition to the shift in position of the loop, residues 52–58 are well ordered in each of the five subunits of the CtxB(H57A) structure. In a large set of previous structures determined for CtxB and EtxB in complex with various receptor analogues, there has been a near perfect correlation of order with sugar binding (19). This has been interpreted as implying that the loop is relatively flexible in the unbound toxin, becoming well ordered as it molds itself around the terminal galactose sugar during receptor binding. In the mutant CtxB(H57A) structure, this correlation is lost, implying that the transition of the loop from a disordered to a fixed structure, which occurs when wild-type B pentamers bind to receptors, has already occurred in the His-57 mutant in the absence of bound saccharide.

Why Does an H57A Mutation in CtxB Attenuate Ctx Action and Ablate B Subunit-Mediated Immunomodulation? It is possible that the H57A mutation subtly alters the nature of interaction with GM1 so that putative, and as yet ill-defined down-stream events cannot be activated. Previous crystallographic studies have revealed that the only structural change that occurs when B pentamers interact with the pentasaccharide of GM1, or with other carbohydrates such as galactose, is that the loop region becomes more rigid (4). Whereas the significance of this has not been explored, it is possible that the transition from a flexible to a rigid structure contributes to the way in which bound GM1 moieties are tethered in the membrane. In this regard, the x-ray crystallography revealed that the loop of the H57A mutant receptor pocket, lacking bound carbohydrate, appeared to have already adopted a more rigid structure. This would therefore preclude the possibility of such a structural transition contributing to GM1 crosslinking in ways that may result in activation of downstream events.

Alternatively, cholera toxin may require interaction, not only with GM1, but also with a coreceptor for it to exert its biological activity. It is conceivable that after binding to GM1, the loops in the B pentamer are positioned to directly interact with other membrane components, possibly a transmembrane protein. Consequently, the alteration in the position of the loops in the B subunit mutants may prevent this from happening, even though the molecule is tethered to the membrane via GM1. Importantly, GM1 is preferentially located in cholesterol-rich detergent-insoluble membrane microdomains, termed ''rafts,'' which contain numerous proteins involved in cell signaling (17). Moreover, there is evidence that rafts contain molecules that interact with the cytoskeleton involved in triggering membrane trafficking (35). Thus, it is conceivable that CtxB binding to GM1 in rafts would position it to interact with signaling and targeting molecules at the membrane surface that participate in toxin-mediated trafficking and immune cell modulation. Preliminary evidence indicates that the His-57 mutation does not interfere with uptake or trafficking in a variety of cell types (S.F. and T.R.H., unpublished results), suggesting that the defect may cause altered signal transduction. If this is correct, it will be important to identify which component at the cell surface interacts with CtxB and whether or not it constitutes an essential coreceptor for toxin action.

We thank Tamera Jones for technical assistance and Drs Lolke de Haan, Simon Hardy, and Lloyd Ruddock for helpful discussions. This work was supported by Medical Research Council Grant G9818467 (to T.R.H.), by National Institutes of Health Grant AI34501 (to W.I.L.), and by the Murdock Foundation and the U.S. Department of Education (to W.G.J.H. and E.A.M.). A.T.A. was supported by the United Kingdom–Indonesia Biodiversity for Biotechnology Development Project (1994–1999) from Department for International Development, and S.F. is the recipient of a Medical Research Council studentship.

1. Hirst, T. R. (1999) in *The Comprehensive Sourcebook of Bacterial Protein Toxins*, eds. Alouf, J. E. & Freer, J. H. (Academic, London), pp. 104–129.
2. Lencer, W. I., Hirst, T. R. & Holmes, R. K. (1999) *Biochim. Biophys. Acta* **1450,** 177–190.
3. Holmgren, J., Lönnroth, I. & Svennerholm, L. (1973) *Infect. Immun.* **8,** 208–214.
4. Sixma, T. K., Kalk, K. H., van Zanten, B. A. M., Dauter, Z., Kingma, J., Witholt, B. & Hol, W. G. J. (1993) *J. Mol. Biol.* **230,** 890–918.
5. Williams, N. A., Hirst, T. R. & Nashar, T. O. (1999) *Immunol. Today* **20,** 95–101.
6. Verweij, W. R., de Haan, L., Holtrop, M., Agsteribbe, E., Brands, R., van Scharrenburg, G. J. M. & Wilschut, J. (1998) *Vaccine* **16,** 2069–2076.
7. Richards, C. M., Aman, A. T., Hirst, T. R., Hill, T. J. & Williams, N. A. (2001) *J. Virol.* **75,** 1664–1671.
8. Sun, J. B., Rask, C., Olsson, T., Holmgren, J. & Czerkinsky, C. (1996) *Proc. Natl. Acad. Sci. USA* **93,** 7196–7201.
9. Williams, N. A., Stasiuk, L. M., Nashar, T. O., Richards, C. M., Lang, A. K., Day, M. J. & Hirst, T. R. (1997) *Proc. Natl. Acad. Sci. USA* **94,** 5290–5295.
10. Bergerot, I., Ploix, C., Petersen, J., Moulin, V., Rask, C., Fabien, N., Lindblad, M., Mayer, A., Czerkinsky, C., Holmgren, J. & Thivolet, C. (1997) *Proc. Natl. Acad. Sci. USA* **94,** 4610–4614.
11. Francis, M. L., Ryan, J., Jobling, M. G., Holmes, R. K., Moss, J. & Mond, J. J. (1992) *J. Immunol.* **148,** 1999–2005.
12. Nashar, T. O., Hirst, T. R. & Williams, N. A. (1997) *Immunology* **91,** 572–578.
13. Nashar, T. O., Webb, H. M., Eaglestone, S., Williams, N. A. & Hirst, T. R. (1996) *Proc. Natl. Acad. Sci. USA* **93,** 226–230.
14. Nashar, T. O., Williams, N. A. & Hirst, T. R. (1996) *Int. Immunol.* **8,** 731–736.
15. Wolf, A. A., Jobling, M. G., Wimer-Mackin, S., Ferguson-Maltzman, M., Madara, J. L., Holmes, R. K. & Lencer, W. I. (1998) *J. Cell Biol.* **141,** 917–927.
16. Orlandi, P. A. & Fishman, P. H. (1998) *J. Cell Biol.* **141,** 905–915.
17. Parton, R. G., Joggerst, B. & Simons, K. (1994) *J. Cell Biol.* **127,** 1199–1215.
18. Merritt, E. A., Sarfaty, S., van den Akker, F., Lhoir, C., Martial, J. A. & Hol, W. G. J. (1994) *Protein Sci.* **3,** 166–175.
19. Merritt, E. A., Sixma, T. K., Kalk, K. H., Van Zanten, B. A. M. & Hol, W. G. J. (1994) *Mol. Microbiol.* **13,** 745–753.
20. Higuchi, R., Krummel, B. & Saiki, R. K. (1988) *Nucleic Acids Res.* **16,** 7351–7367.
21. Rodighiero, C., Aman, A. T., Kenny, M. J., Moss, J., Lencer, W. I. & Hirst, T. R. (1999) *J. Biol. Chem.* **274,** 3962–3969.
22. Furste, J. P., Pansegrau, W., Frank, R., Blocker, H., Scholz, P., Bagdasarian, M. & Lanka, E. (1986) *Gene* **48,** 119–131.
23. Hirst, T. R., Randall, L. L. & Hardy, S. J. S. (1984) *J. Bacteriol.* **157,** 637–642.
24. Ruddock, L. W., Ruston, S. P., Kelly, S. M., Price, N. C., Freedman, R. B. & Hirst, T. R. (1995) *J. Biol. Chem.* **270,** 29953–29958.
25. Merritt, E. A., Kuhn, P., Sarfaty, S., Erbe, J. L., Holmes, R. K. & Ho, W. G. J. (1998) *J. Mol. Biol.* **282,** 1043–1059.
26. Otwinowski, Z. & Minor, W. (1997) *Methods Enzymol.* **276,** 307–326.
27. Bailey, S. (1994) *Acta Crystallogr. D* **50,** 760–763.
28. McRee, D. (1993) *Practical Protein Crystallography* (Academic, San Diego).
29. Sanner, M. F., Olson, A. J. & Spehner, J. C. (1996) *Biopolymers* **38,** 305–320.
30. Merritt, E. A. & Bacon, D. J. (1997) *Methods Enzymol.* **277,** 505–524.
31. Lencer, W. I., Delp, C., Neutra, M. R. & Madara, J. L. (1992) *J. Cell Biol.* **117,** 1197–1209.
32. Hardy, S. J. S., Holmgren, J., Johansson, S., Sanchez, J. & Hirst, T. R. (1988) *Proc. Natl. Acad. Sci. USA* **85,** 7109–7113.
33. Sandkvist, M., Hirst, T. R. & Bagdasarian, M. (1990) *J. Biol. Chem.* **265,** 15239–15244.
34. Kuziemko, G. M., Stroh, M. & Stevens, R. C. (1996) *Biochemistry* **35,** 6375–6384.
35. Badizadegan, K., Wolf, A., Rodighiero, C., Jobling, M. G., Hirst, T. R., Holmes, R. K. & Lencer, W. I. (2000) *Int. J. Med. Microbiol.* **290,** 403–408.